

## ARTICLE

# Characterization of Apparently Balanced Chromosomal Rearrangements from the Developmental Genome Anatomy Project

Anne W. Higgins,<sup>1</sup> Fowzan S. Alkuraya,<sup>2</sup> Amy F. Bosco,<sup>3</sup> Kerry K. Brown,<sup>4</sup> Gail A.P. Bruns,<sup>5</sup> Diana J. Donovan,<sup>1</sup> Robert Eisenman,<sup>5</sup> Yanli Fan,<sup>2</sup> Chantal G. Farra,<sup>1</sup> Heather L. Ferguson,<sup>3</sup> James F. Gusella,<sup>4,6</sup> David J. Harris,<sup>7</sup> Steven R. Herrick,<sup>1</sup> Chantal Kelly,<sup>3</sup> Hyung-Goo Kim,<sup>6</sup> Shotaro Kishikawa,<sup>6</sup> Bruce R. Korf,<sup>8</sup> Shashikant Kulkarni,<sup>9</sup> Eric Lally,<sup>1</sup> Natalia T. Leach,<sup>3</sup> Emma Lemyre,<sup>10</sup> Janine Lewis,<sup>6</sup> Azra H. Ligon,<sup>1</sup> Weining Lu,<sup>11</sup> Richard L. Maas,<sup>2</sup> Marcy E. MacDonald,<sup>6,12</sup> Steven D.P. Moore,<sup>3</sup> Roxanna E. Peters,<sup>1</sup> Bradley J. Quade,<sup>1</sup> Fabiola Quintero-Rivera,<sup>6</sup> Irfan Saadi,<sup>2</sup> Yiping Shen,<sup>6</sup> Jay Shendure,<sup>4</sup> Robin E. Williamson,<sup>4,13</sup> and Cynthia C. Morton<sup>1,3,13,\*</sup>

Apparently balanced chromosomal rearrangements in individuals with major congenital anomalies represent natural experiments of gene disruption and dysregulation. These individuals can be studied to identify novel genes critical in human development and to annotate further the function of known genes. Identification and characterization of these genes is the goal of the Developmental Genome Anatomy Project (DGAP). DGAP is a multidisciplinary effort that leverages the recent advances resulting from the Human Genome Project to increase our understanding of birth defects and the process of human development. Clinically significant phenotypes of individuals enrolled in DGAP are varied and, in most cases, involve multiple organ systems. Study of these individuals' chromosomal rearrangements has resulted in the mapping of 77 breakpoints from 40 chromosomal rearrangements by FISH with BACs and fosmids, array CGH, Southern-blot hybridization, MLPA, RT-PCR, and suppression PCR. Eighteen chromosomal breakpoints have been cloned and sequenced. Unsuspected genomic imbalances and cryptic rearrangements were detected, but less frequently than has been reported previously. Chromosomal rearrangements, both balanced and unbalanced, in individuals with multiple congenital anomalies continue to be a valuable resource for gene discovery and annotation.

## Introduction

Approximately 1 in 2000 newborns has a de novo balanced chromosomal rearrangement.<sup>1</sup> Although the majority of these individuals will have no discernible clinical phenotype, the risk for a congenital anomaly in this population is two to three times higher than that observed in an unselected population of newborns, for which the risk of anomalies is 2%–3%.<sup>1</sup> Clinical findings observed in patients with such chromosomal rearrangements are thought to be caused by disruption or dysregulation of a gene (or genes) at or near the breakpoint. The underlying pathogenetic mechanism may result from an intragenic break,<sup>2,3</sup> from accompanying genomic copy alterations at or in the vicinity of the breakpoint,<sup>4</sup> from production of a chimeric gene,<sup>5</sup> or from a position effect on a gene (or genes) distant from the breakpoint.<sup>6</sup> In addition, chromosomal rearrangements may disrupt noncoding RNA genes or conserved nongenic

sequences, two elements whose roles in genome architecture and gene regulation have yet to be elucidated fully.<sup>7,8</sup> The resulting physiological consequences can include complete abrogation of the protein if the corresponding allele is imprinted or otherwise mutated, haploinsufficiency, elevated expression, or creation of a fusion protein with a dominant-negative effect or novel gain of function.

Use of chromosomal rearrangements as signposts for genes important in human disease is well documented.<sup>9–15</sup> Historically, these chromosomal rearrangements were investigated with conventional cytogenetic banding methods and subsequent arduous positional-cloning projects. More recently, molecular cytogenetic characterizations using labeled DNA from bacterial artificial chromosomes (BACs) in fluorescence in situ hybridization (FISH) and array comparative genomic hybridization (aCGH) studies have allowed more precise and rapid localization of breakpoints. Recent studies of patients with phenotypic

<sup>1</sup>Department of Pathology, Brigham and Women's Hospital and Harvard Medical School, Boston, MA 02115, USA; <sup>2</sup>Division of Genetics, Department of Medicine, Brigham and Women's Hospital, Boston, MA 02115, USA; <sup>3</sup>Department of Obstetrics, Gynecology and Reproductive Biology, Brigham and Women's Hospital and Harvard Medical School, Boston, MA 02115, USA; <sup>4</sup>Department of Genetics, Harvard Medical School, Boston, MA 02115, USA; <sup>5</sup>Genetics Division, Department of Pediatrics, Children's Hospital Boston and Harvard Medical School, Boston, MA 02115, USA; <sup>6</sup>Molecular Neurogenetics Unit, Center for Human Genetic Research, Massachusetts General Hospital and Department of Genetics, Harvard Medical School, Boston, MA 02114, USA; <sup>7</sup>Division of Genetics, Children's Hospital Boston and Harvard Medical School, Boston, MA 02115, USA; <sup>8</sup>Department of Genetics, University of Alabama at Birmingham, Birmingham, AL 35294, USA; <sup>9</sup>Division of Laboratory and Genomic Medicine, Department of Pathology, Washington University School of Medicine, St Louis, MO 63110, USA; <sup>10</sup>Medical Genetics Division, Hôpital Ste. Justine, University of Montreal, Montreal H3T 1C5, Canada; <sup>11</sup>Renal Section, Department of Medicine, Boston University Medical Center, Boston, MA 02118, USA; <sup>12</sup>Department of Neurology, Harvard Medical School, Boston, MA 02114, USA

<sup>13</sup>All editorial responsibility for this article was handled by an associate editor of the *Journal*.

\*Correspondence: [cmorton@partners.org](mailto:cmorton@partners.org)

DOI 10.1016/j.ajhg.2008.01.011. ©2008 by The American Society of Human Genetics. All rights reserved.

abnormalities and chromosomal rearrangements used the above methods and have revealed that some presumably balanced rearrangements include cryptic deletions or more complex rearrangements.<sup>16,17</sup> However, these investigations have examined relatively small numbers of patients and have not specifically studied the breakpoints at the level of the DNA sequence.

In this study, we describe the comprehensive examination of 40 reportedly balanced chromosomal rearrangements from patients with clinical abnormalities. These patients were ascertained through the Developmental Genome Anatomy Project (DGAP). DGAP is a multidisciplinary study bringing together cytogeneticists, molecular biologists, and developmental biologists to understand the genetic basis of birth defects and the underlying molecular basis of development. This goal is pursued through the study of individuals with apparently balanced chromosomal rearrangements who also have major congenital anomalies. Through leveraging of the resources generated by the Human Genome Project, the breakpoints of these rearrangements can be mapped expeditiously to discover and annotate genes likely to be critical in mammalian development.

As a consequence of this effort, we characterized 77 breakpoints from 40 chromosomal rearrangements by using FISH with BACs and fosmids, array CGH, Southern-blot hybridization, multiplex ligation-dependent probe amplification (MLPA), RT-PCR, and suppression PCR. Eighteen chromosomal breakpoints were cloned and sequenced. Herein we report the detailed analyses of these rearrangements including identification of cryptic copy-number alterations and complex rearrangements.

## Material and Methods

### Patients and Cell Lines

Individuals were enrolled in the DGAP study after identification of an apparently balanced chromosomal rearrangement and at least one clinically significant congenital anomaly (e.g., cleft lip). All human study protocols were reviewed and approved by the Partners Health Care System Human Research Committee. Lymphocyte cell transformation was performed at the Massachusetts General Hospital Genomics Core Facility in the Center for Human Genetic Research (Boston, MA). Cell lines prepared from individuals with similar phenotypic and cytogenetic criteria were obtained from the National Institute of General Medical Sciences (NIGMS) Human Genetic Cell Repository (Coriell Cell Repositories, Camden, NJ).

### Cytogenetic Analysis

Metaphase chromosomes were prepared from lymphoblastoid cell lines or fibroblast cultures according to routine protocols. Chromosomes were GTG banded via standard methods, and at least ten metaphase spreads were examined per patient. Resolution for the GTG-banded chromosomes was  $\geq 550$  bands.

### Probes for Fluorescence In Situ Hybridization

BACs for breakpoint mapping of chromosomal rearrangements were selected with the University of California Santa Cruz Genome Browser and Database and the NCBI Human Genome Browser and

Database. BACs from the RP1, RP3, RP4, RP5, RP6, RP11, and RP13 libraries and fosmids from the wi2 library were obtained from Children's Hospital Oakland Research Institute (CHORI, Oakland, CA). BACs from the CTB, CTC, and CTD libraries were obtained from Invitrogen (Carlsbad, CA). DNA was isolated in accordance with a standard protocol consisting of alkaline lysis, neutralization, and ethanol precipitation (QIAGEN, Valencia, CA). Polymerase chain reaction (PCR) fragments were generated by routine methods. PCR fragments were either gel purified with the QIAquick Gel Extraction Kit (QIAGEN) or purified with the QIAquick PCR Purification Kit (QIAGEN). Isolated DNA was labeled directly with either SpectrumGreen- or SpectrumOrange-conjugated dUTP, via the Nick Translation Reagent Kit from Abbott Molecular/Vysis (Des Plaines, IL), or indirectly with biotin or digoxigenin via the DIG DNA Labeling Kit or Biotin DNA Labeling Kit (Roche Diagnostics, Indianapolis, IN). Cot-I DNA was added to suppress repetitive sequences, and probes were ethanol precipitated and resuspended in Hybrisol containing 50% formamide (Abbott Molecular/Vysis).

### Fluorescence In Situ Hybridization

Metaphase chromosome preparations from each DGAP case were prepared on glass slides in accordance with standard hypotonic lysis and fixation, followed by dehydration in a series of ethanol washes and probe application. Both probes and chromosomes were denatured simultaneously at 72°C for 2 min and incubated overnight at 37°C in a HYBrite apparatus (Abbott Molecular/Vysis). Slides were washed in 50% formamide/2×SSC at 37°C for 20 min and 2×SSC at 37°C for 20 min. 4',6'-diamidino-2-phenylindole hydrochloride (DAPI) was used as counterstain. Hybridization results were assessed with a Zeiss Axioskop 2 epifluorescence microscope (Thornwood, NY) or an Olympus BX51 microscope (Center Valley, PA), and images were acquired with an Applied Imaging CytoVision cytogenetics workstation (Santa Clara, CA). A minimum of ten metaphases were scored per probe (set).

### Array Comparative Genomic Hybridization

aCGH was performed with either Spectral Genomics 2600 BAC arrays (Houston, TX) with an ~1 Mb resolution or Agilent Technologies 244K (G4411B) oligonucleotide arrays consisting of 60-mer oligonucleotides spaced at 8.9 kb (Santa Clara, CA).

### Southern-Blot Analysis

Southern blotting was performed by standard methods. BAC sequences of breakpoint critical regions were examined with Repeat Masker to identify regions from which unique probes could be generated. Genomic DNA probes of ~200 to ~1500 base pairs (bp) were prepared from these nonrepetitive sequences by PCR. PCR products were labeled with the Megaprime DNA labeling Kit (Amersham Biosciences, Piscataway, NJ). Aberrant bands detected in patient samples but absent in control samples indicated localization of the breakpoint within these restriction fragments.

### Breakpoint Cloning

Rearrangement breakpoints were cloned via modifications of the suppression PCR protocol<sup>18</sup> as described.<sup>19</sup> Cloned junction fragments were sequenced by standard methods.

### Fusion Transcript Amplification

Fusion transcript amplification was performed with RT-PCR according to routine protocols. Primer sequences are previously described.<sup>2,20</sup>

## Candidate-Gene Transcript Analysis

Gene dosage of selected candidate genes was investigated with MLPA as described.<sup>21</sup>

## Analysis of Sequence Motifs at Breakpoint Regions

Eighteen sequenced breakpoints (from DGAP cases 003, 011, 012, 032, 090, 097, 105, 107, and 151) were used for this analysis. A nonredundant set of sequences, consisting of 15 bp upstream and downstream of each breakpoint (i.e., 30 to 60 bp per breakpoint, depending on the presence and length of deletions at the breakpoint itself), were extracted and used for analysis. This yielded 841 bp of breakpoint-associated sequence. A Poisson distribution was used to evaluate whether an excess of observations of each motif was present in the breakpoint-associated sequence. For each evaluated motif, background frequencies were estimated by their frequency of occurrence in an arbitrary 1 Mb of human genomic sequence (from chromosome 10).

## Results

Samples were obtained from individuals with a wide spectrum of anomalies, and no specific anomaly or organ system was the focus of enrollment in the DGAP study. Phenotypes of DGAP cases include physical findings such as cleft lip and palate, neurological impairments such as obsessive-compulsive disorder, and multisystem abnormalities (Figure 1 and Table 1).

## Breakpoint Mapping

Cell lines established from individuals enrolled in DGAP were examined initially with FISH with BAC probes to define the genomic region of the breakpoints. A series of iterative experiments with clones in the region was performed until one clone produced a "split signal." A genomic clone was determined to contain the breakpoint if signals were observed on the normal chromosome and both derivative chromosomes. Through the use of overlapping end-sequenced BAC clones and smaller probes, such as fosmids and PCR fragments, breakpoint critical regions were narrowed further to as small a region as 0.4 kilobases (kb).

As a result of the FISH analyses, the initial reported karyotype designations determined by GTG banding were revised for 18 of the 40 chromosomal rearrangements. For all but one rearrangement, the refined breakpoint shifted to the adjacent GTG band or next most adjacent GTG band. This finding is not surprising given the lower resolution of GTG banding compared with FISH and the relatively subjective nature of breakpoint designation via GTG banding. For the single case in which the breakpoints mapped were substantially different from those reported, the GTG-banded karyotype was reviewed and the FISH-based breakpoint assignments confirmed.

FISH analyses also revealed that a number of DGAP cases have deletions (Table 2). Deletions ranging in size from ~500 kb to 12 megabases (Mb) were found in 15 of 40 DGAP cases analyzed. The majority of these deletions mapped to the breakpoints, although five (DGAP089, 159, 169,

174, and 200) mapped at a distance from the breakpoint and one (DGAP107) was completely independent of the breakpoint. Three cases (DGAP106, 159, 169) had deletions at both breakpoints. The 12 Mb deletion seen in DGAP089 was reported to us during the course of our study by the submitting geneticist after detection by conventional (metaphase) CGH.<sup>22</sup> This finding was confirmed and the boundaries of the deletion were refined by Spectral Genomics 2600 BAC aCGH.<sup>23</sup> In the case of the DGAP107 deletion, the referring physician reported a serendipitous discovery of a deletion in the Smith-Magenis syndrome critical region during a laboratory study of patients with sleep disturbances; DGAP107 had been selected as a control specimen for probe validation. Once this deletion was reported to us, the deletion interval was verified by FISH.<sup>20</sup>

We identified only two complex rearrangements among this reported series of DGAP cases. DGAP018 had a reported karyotype of 46,XX,ins(3;1)(q23;p22p32). FISH analysis with five BACs that mapped to 1p32 through 1p21 hybridized to what appeared to be a derivative chromosome 2, der(2). Multiplex FISH (M-FISH) was performed and revealed that material from chromosome 1 was inserted into the short arm of chromosome 2, and material from chromosome 2 was inserted into the long arm of chromosome 3. FISH experiments using BACs localized to the interval of chromosome 2p14 to 2p16-p21 suggested that this interval is duplicated and inserted into chromosome 3. In the second case, DGAP122, a complex rearrangement was reported between chromosomes 1, 5, and 9, and the karyotype was revised to the following: 46,XY,t(1;9;5)(1pter→1q32::9p22-24::5q15→5qter;9pter→9p24::9p22→9qter;5pter→5q15::1q32→1qter). FISH analysis of this case revealed even further rearrangements with multiple possible duplications.

In addition to FISH analyses, selected cases were analyzed with aCGH (Table 3). Eleven cases were examined with either Spectral Genomics 2600 BAC arrays or Agilent Technologies 244K oligonucleotide arrays, and one case was examined with both. Five cases showed no additional rearrangements. Six cases showed copy-number losses ranging in size from 0.5 Mb to ~12 Mb. The 12 Mb loss seen in DGAP089 was observed cytogenetically, and the array experiment refined the boundaries of the deletion. No cases had copy-number gains by array analysis.

After breakpoint regions were narrowed to a minimum region of ~20 kb with FISH probes, Southern-blot analysis was performed for 15 breakpoints. These breakpoints were pursued beyond the limits of FISH analysis because they harbored the most promising candidate genes in the vicinity of the FISH-mapped breakpoint. Breakpoint localization by Southern blotting revealed slight discrepancies between the localization predicted by FISH mapping and the Southern-blot analysis in six cases. These six breakpoints were localized outside the FISH-defined region by an interval ranging from 6 to 32 kb. In one case, DGAP100, the cloned breakpoint was 8 kb from the terminus within

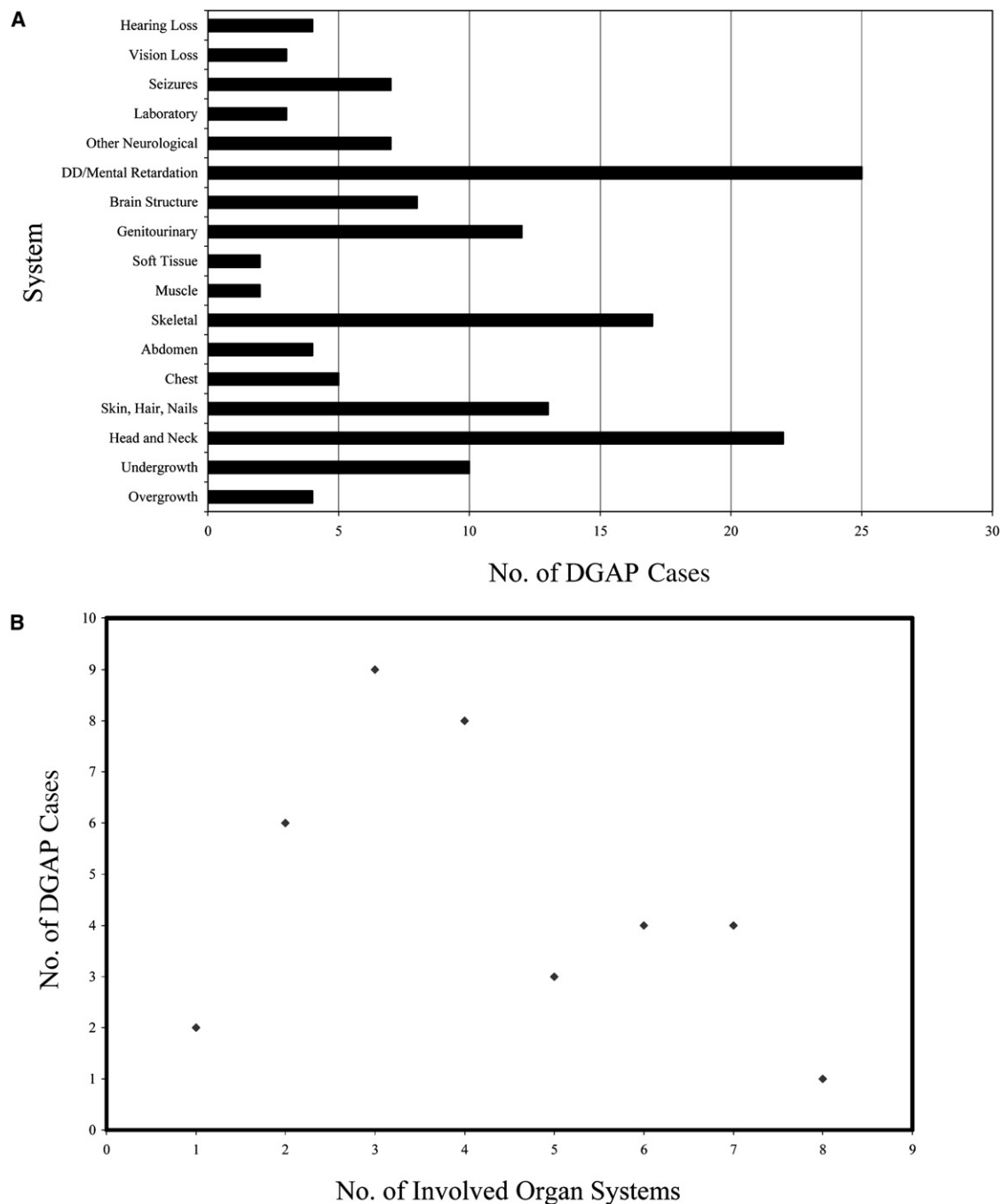


**Figure 1. Complexity of DGAP Phenotypes**

(A) The multiple systems involved in DGAP cases illustrate the complexity of phenotypes observed.

(B) Most individuals studied have malformations of multiple systems, ranging from one to eight systems.

a BAC clone that did not show a split hybridization signal on metaphase chromosomes. This example demonstrates the intrinsic difficulty in detecting hybridization to both derivative chromosomes when the breakpoint is located at the corresponding end of the FISH probe. Unequal distribution of repetitive and single-copy sequences in the BAC probe could create the same difficulty. Use of smaller probes such as fosmids and PCR products may help to minimize such discrepancies. Our strategy to clone the break-

points incorporates this information by screening for a breakpoint in the 10 to 30 kb genomic segment flanking the FISH-defined region.

After breakpoint regions were localized to single restriction fragments, suppression PCR was used to amplify junction sequences.<sup>18</sup> These PCR products were then cloned and sequenced. With this approach, eighteen breakpoints have been cloned and sequenced from nine chromosomal rearrangements (Table 4).

**Table 1. Phenotype and Karyotype of Selected DGAP Cases**

Case No.	Phenotype	Karyotype	Publication
DGAP003	Delayed dentition, gingival hyperplasia, hirsutism, large facial bones and mandibles, large ears, a markedly enlarged nose with short columella nasi and saddle deformity, depressed nasal bridge, hypertelorism with bilateral convergent strabismus, epicanthal folds, protruding upper lip, hypertrophic papillae on the posterior of the tongue, bilateral spade-like fingers, skin thickening on the legs, dysmorphic skeletal features	46,XY,t(3;17)(p14.3;q24.3)dn	21, 33
DGAP006	Mental retardation, developmental delay, absent speech, aggressive behavior, frontal bossing, epicanthal folds, left eye ptosis, low-set ears, no binocular fixation searching movements	46,XX,t(1;2)(p32;q11)dn	
DGAP009	Mental retardation, eye anomaly, other multiple congenital anomalies	46,XY,t(1;8)(p34;q22)dn	2
DGAP011	Kallmann syndrome (atrophic testes, azoospermia, cleft lip and palate)	46,XY,t(7;8)(p12.3;p11.2)dn	
DGAP012	Developmental delay, digitalized thumbs, brachycephaly, microcephaly, small down-turned mouth, mild midfacial hypoplasia, flat mid-face, narrow nasal bridge, very small nose, large ears, bilateral epiblepharon without trichiasis, small hands and feet, absence of emotional expression, hand flapping, early feeding problems	46,XY,t(11;19)(p11.2;p13.2)dn	
DGAP015	Bannayan-Riley-Ruvalcaba syndrome, malignant intracranial hCG-secreting tumor causing precocious puberty	46,XY,t(10;13)(q23.3;q33)dn	
DGAP016	Hypoplastic testes	46,XY,t(8;10)(p11.2;p13)dn	
DGAP018	Bilateral osseocutaneous syndactyly of the 3rd, 4th, and 5th fingers; hypotonia; macrocephaly; forehead and occipital prominence; left inner thigh hemangioma; developmental delay	46,XX,?dup(2)(p14p?21),ins(2;1)(?p13;p21p31),ins(3;2)(q23;p14p?21)dn	
DGAP020	Sex reversal, gonadoblastoma, streak gonad, amenorrhea	46,X,t(Y;17)(q11;p13)dn	
DGAP025	Developmental delay, scoliosis, syndactyly of toes, learning problems, masculinized face, hirsutism	46,X,t(X;15)(p22;q26)dn	
DGAP032	Kallmann syndrome (hypogonadotropic hypogonadism, and anosmia), skeletal anomalies, mental retardation	46,XY,t(7;12)(q21.13;q24)dn	
DGAP089	Subarachnoid hemorrhage, ventriculomegaly, underdeveloped corpus callosum, tonic-clonic seizure, severe delays in growth and development, craniofacial disproportion and dysmorphism, right cryptorchidism, hypotonia, chronic intestinal obstruction	46,XY,t(1;2)(p31.3;q22.1), del(2)(q14.3q21)dn	23
DGAP090	Sensorineural hearing loss, Mondini defect, avascular necrosis of the left femoral head, dermal telangiectasias with ulceration, juvenile rheumatoid arthritis	46,XY,t(8;9)(q12.1;p21.3), t(9;11)(q33;q13)mat	34
DGAP095	Seizures, developmental delay, infantile hypotonia, obesity, <i>livedo reticularis</i>	46,X,t(X;2)(p11.2;q37)dn	32
DGAP097	Developmental delay, infantile spasms, hypotonia, mental retardation, behavioral problems, facial dysmorphism, myopia, patchy skin hypopigmentation	46,X,t(X;9)(p22.2;p13)dn	
DGAP100	Mental retardation, severe psychomotor delay, mild ventriculomegaly, failure to thrive, no speech, no ambulation, cleft palate, impaired hearing, bilateral optic nerve hypoplasia, severe myopia, hypoglycemia, mild pectus excavatum, gray teeth with caries	46,X,t(X;5)(p11.23;q35)dn	
DGAP101	Severe mental retardation, no speech, mild dysmorphism, clinodactyly, mild hirsutism	46,XY,inv(5)(q13q15)dn	
DGAP103	Extreme somatic overgrowth, advanced endochondral bone and dental ages, a cerebellar tumor, multiple lipomas	46,XY,inv(12)(p11.22q14.3)dn	3
DGAP104	Congenital hydrocephalus, abnormal corpus callosum, periventricular calcifications, sacral anomaly, hypoplastic kidneys	46,XX,t(1;20)(p31.3;q13.31)dn	23
DGAP105	Aortic coarctation; bicuspid aortic valve; bilateral cryptorchidism and primary hypospadias; inguinal hernia; widely spaced nipples; short neck; four hair whorls (three posterior and one anterior); down-slanting palpebral fissures; bilateral epicanthal folds; broad nose; smooth philtrum; thin vermilion border; low-set and posteriorly rotated ears with simplified, thickened helices; mild hypertelorism and strabismus; developmental delay	46,XY,t(1;5)(p35.3;q31.3)dn	
DGAP106	Developmental delay, self-injurious actions and agitation, growth retardation, strabismus, ptosis, normal MRI	46,XX,t(3;5)(q27;q31.1), t(11;13)(p15.3;q14.1)dn	20
DGAP107	Visual defects, limb defects, urinary tract abnormalities, learning disabilities, genital anomalies, neurological and behavioral defects	46,XY,t(Y;3)(p11.2;p12.3)dn	



**Table 1. Continued**

Case No.	Phenotype	Karyotype	Publication
DGAP112	Microcephaly, advanced bone age and secondary craniosynostosis, developmental delay, flat nasal bridge, epicanthal folds, strabismus, short philtrum, thin upper lip, two café-au-lait spots, 2nd toes overlap 3rd toes bilaterally, small labia majora, extra creases on right hand, wide thumbs and halluces	46,XX,t(3;12)(q13.2;q14), del(12)(q14q14)dn	
DGAP121	Feeding problems at birth, malformed left ear lobe, epicanthal folds, learning problems, mild hypotonia, mild resolved scoliosis	46,XX,t(5;13)(q15;q32)dn	
DGAP122	Epicanthal folds; hypertelorism; frontal and posterior cowlick; coarse hair; area of alopecia; history of patchy, intermittent hair loss; partially attached pinnae; mild micrognathia; mild pectus excavatum; soft systolic murmur with normal echocardiogram; developmental delay; renal insufficiency caused by grade II-III hydronephrosis	46,XY,t(1;9;5)(1pter→1q32:: 9p22-24::5q15→5qter;9pter→ 9p24::9p22→9qter;5pter→ 5q15::1q32→1qter)dn*	
DGAP123	Autism	46,XX,ins(16;2)(q22.1;p16.1p16.3) pat.ish ins(16;2)(wcp2+;wcp2+)	36
DGAP127	Failure to thrive; feeding problems; growth retardation; unexplained weight loss; brachycephaly; flat mid-face; pointed chin; broad, prominent forehead; deeply set eyes; small mouth; frequent episodes of abdominal pain; some difficulties with reflux; kidney stones; developing contractures and spasticity of the ankles, knees, elbows and shoulders; severe developmental delay; very poor eye contact/interaction; self-stimulating episodes; episodic discomfort and agitation with no apparent cause; seizures; muscle biopsy demonstrated partial complex III deficiency	46,X,t(X;5)(q24;q13)dn	
DGAP128	Macrocephaly, significant developmental delay, seizures and cerebral atrophy	46,XX,t(1;3)(q32.2;q25.2)dn	35
DGAP137	Mild mental retardation, pigment abnormality, VSD, conductive hearing loss, abnormal thyroid function tests, right eye poor visual acuity (small pit in right optic nerve), bilateral optic nerve colobomas, MRI shows 1.5 cm mass behind right globe (no enhancement), bulbous great toes with convex toenails, ligamentous laxity, easy bruising	46,XX,der(6)t(6;13)(q23.3;q22) inv(6)(p21.3q15),der(13)t(6;13)dn	
DGAP139	Developmental delay; hypotonia; dolicocephaly; frontal upsweep; synophrys; long, straight eyelashes; small nares; pronounced philtral creases; small mouth; flat hemangiomas on back of neck; pectus excavatum; joint hyperextensibility; feet have increased secondary creases on both soles; hands have a right Sydney line	46,XY,t(7;13)(p15.3;q14.1)dn	
DGAP151	Cleft lip and palate	46,XX,t(2;8)(q33.1;q24.3)dn	19
DGAP157	Global developmental delay, bilateral inguinal hernia, spina bifida occulta, mild dysmorphic features	46,XY,t(3;10)(p26.3;q26.3)dn	
DGAP159	Growth retardation, brachydactyly, bilateral syndactyly of 2nd and 3rd toes, micrognathia, low-set ears, hypertelorism and single palmar crease, developmental delay, no oral language, some autistic and ADD behaviors, abnormal brain CT (5 months of age), moderate to severe bilateral conductive hearing loss, hypo and hypersensitive to different tactile stimulation, trouble focusing eyes on close objects	46,XY,t(8;10)(q13;p13)dn	
DGAP166	Seizure disorder, developmental delay, microcephaly, bilateral epicanthal folds, nose upturned with a thin upper lip and upturned corners of the mouth, very mild micrognathia	46,XX,inv(2)(p23q31)dn	
DGAP167	Mild developmental delay, vertical talus (rocker-bottom foot deformity), hypotonia	46,XX,inv(18)(q11.2q23)dn	
DGAP169	Failure to thrive, feeding problems, growth retardation, bilateral microtia with profound sensorineural deafness, fused incus and malleus, incus with absent short process, bilateral Mondini malformation, abnormal cochlear turn, malformation of the semicircular canals, micrognathia, anteriorly displaced larynx, small right kidney with renal cortical thinning, borderline wide interpedicular distance of C-spine (18 mm C7, 15–16 mm C5), developmental delay, abnormal hair distribution with high forehead, benign precocious thelarche at 9 months that resolved by 15 months	46,XX,inv(5)(q14q35)dn	

*(Continued on next page)*

**Table 1. Continued**

Case No.	Phenotype	Karyotype	Publication
DGAP173	Mild developmental delay; major depression; generalized anxiety; sleep apnea; self-injurious behaviors; agitation; tantrums; overgrowth; male-pattern hirsutism; amenorrhea; impaired glucose tolerance; hypercholesterolemia and hypertriglyceridemia; elevated testosterone; deep voice; history of one seizure at 2 yr of age; eczema; acanthosis nigricans; moles and skin tags; bilateral epicanthal folds; small nose; complex malocclusion; short, hyperkeratotic palms; 5th finger brachydactyly and clinodactyly; right elbow extension limitation; hypoplastic toenails; short feet	46,XX,t(2;11)(q11.2;p13)dn	
DGAP174	Overgrowth, right-sided hemihypertrophy, small apical VSD and current heart murmur, metopic craniosynostosis and hydrocephalus, Arnold Chiari II malformation, agenesis of the corpus callosum, dysplasia of the left temporal lobe, scoliosis, developmental delay, attention deficit hyperactivity disorder, increased red blood cell size, asthma and seasonal allergies, left inguinal hernia that was surgically repaired, bilateral epicanthal folds, slight occasional esotropia, high-arched palate, left-sided head tilt, unsteady gait and uncoordinated movements with decreased balance	46,XY,t(1;3)(p22;q21), del(1)(p31.3p32.1)dn	23
DGAP190	Developmental delay, infantile spasms	46,XX,t(X;8)(p22;p21)dn	
DGAP200	PDD-NOS, ADHD, conduct disorder with early onset, intermittent explosive disorder, obesity	46,XY,t(1;2)(q31.3;p16.3)dn	36

\*indicates reported karyotype; FISH analyses suggest additional rearrangements that were not characterized further.

### Breakpoint Sequence Analysis

We examined the genomic architecture of the breakpoint regions. Analysis of the 18 cloned breakpoints revealed 11 microdeletions of 1–16 bp, six insertions of 2–17 bp, two duplications of 3 and 13 bp, and four rearrangements without gain or loss of a nucleotide at one or more breakpoints. Three of the 18 breakpoints showed multiple types of sequence changes including deletion and insertion or duplication (Table 4). In one case (DGAP011), both breakpoints were perfectly balanced (i.e., no loss or gain of sequence on either derivative chromosome). In eight cases, breakpoints fell within repetitive sequences including three LINE, three Alu/SINE, and two LTR elements. Inter-

estingly, both breakpoints in DGAP095 contain AluSx elements, possibly facilitating formation of this rearrangement via illegitimate recombination.

To explore a possible common mechanism of formation of the chromosomal rearrangements studied, we searched for possible common sequence motifs at the breakpoints. We first evaluated 37 motifs listed by Abeyasinghe et al. in their analyses of 235 sequences.<sup>24</sup> These motifs either had previously been noted to be present at rearrangement breakpoints or are associated with mechanisms (e.g., recombination) that might be etiologic in a rearrangement. Several of the sequence motifs were reported in that study to be overrepresented at translocation breakpoints. In contrast, we found that none of these 37 sequence motifs was significantly overrepresented in our set of breakpoint sequences after correcting for multiple-hypothesis testing. It is possible that the number of breakpoints assessed in our study was insufficient to replicate the findings of the previous study. However, breakpoint sequences analyzed by Abeyasinghe et al. were primarily derived from malignancies, rather than de novo germline rearrangements, and a different molecular mechanism may reasonably underlie their origin.<sup>24</sup>

As a more comprehensive search, we tested partially degenerate 8-mer motifs by the same method, in which each motif consisted of six fixed positions and two degenerate positions (e.g., AGAGNAGN). After testing of the full set of possibilities for sequence motifs with this structure, none was found to be overrepresented in the breakpoint sequences after correcting for multiple-hypothesis testing.

Submission of the breakpoint sequences to the YMF 3.0 motif-finding tool yielded ATWAGGRA as the top-scoring motif, with five occurrences, but the significance of this

**Table 2. Deletion Size and Location in DGAP Cases**

Case No.	Deletion Size	Location
DGAP009	1.5 Mb	At breakpoint
DGAP020	900 kb	At breakpoint
DGAP089	~12 Mb	~3 Mb from breakpoint
DGAP106	≥1.5 Mb	At breakpoint
DGAP106	500 - 800 kb	At breakpoint
DGAP107	3.4 Mb	Different chromosome
DGAP112	750 kb	At breakpoint
DGAP137	226 kb - 1.9 Mb	At breakpoint
DGAP139	600 kb	At breakpoint
DGAP159	3 Mb	~1.75 Mb from breakpoint
DGAP159	6 Mb	At breakpoint
DGAP167	8 Mb	At breakpoint
DGAP169	500 kb	200 kb from breakpoint
DGAP169	500 kb	At breakpoint
DGAP173	2.5 Mb	At breakpoint
DGAP174	2.2 Mb	~10 Mb from breakpoint
DGAP190	~4 Mb	At breakpoint
DGAP200	~500 kb	~2 Mb from breakpoint

**Table 3. Array Comparative Genomic Hybridization Analyses of Selected DGAP Cases**

Case No.	Imbalance	Flanking BACs	Region of Imbalance	~Size of Imbalance in Mb	Platform <sup>a</sup>
DGAP089	LOSS	RP11-270M20, RP11-472M4	RP11-294I11 to RP11-289K3	12	SG
DGAP107	LOSS	<i>ZNF287</i> , <i>DKFZp5660084</i> <sup>b</sup>	<i>LOC201164</i> to <i>AKAPP10</i> <sup>b</sup>	3.4	SG,AT
DGAP159	LOSS	RP11-659E9, RP11-212P10	RP11-288G19 to RP11-346i3	3.0	SG
DGAP159	LOSS	RP11-287021, RP1174N14	RP11-91K20 to RP11-80D10	6.0	SG
DGAP173	LOSS	RP11-16H3, RP1-296L11	RP11-79M22 to RP11-79E9	2.5	SG
DGAP174	LOSS	RP11-63G10, RP11-5P4	RP11-13N22 to RP4-662P1	2.2	SG
DGAP200	LOSS	<i>BC005076</i> , <i>SPTBN1</i> <sup>b</sup>	<i>ACYP2</i> to <i>SPTBN1</i> <sup>b</sup>	0.5	AT
DGAP003	NONE	—	—	—	AT
DGAP028	NONE	—	—	—	AT
DGAP095	NONE	—	—	—	SG
DGAP104	NONE	—	—	—	SG
DGAP151	NONE	—	—	—	SG

<sup>a</sup> SG = Spectral Genomics 2600 BAC array, AT = Agilent Technologies 244K (G4411B).

<sup>b</sup> 60-mer oligonucleotides based on sequence from the genes listed.

motif is uncertain because it is unclear how many hypotheses are tested by this algorithm. Further testing of this motif as a specific hypothesis can be performed as additional examples of breakpoint sequences are determined.

Forty-seven breakpoints from 27 cases were positioned and examined for candidate genes. Genes were directly disrupted by 34 breakpoints (Table 4): 22 within introns (ranging in size from 2.9 to 379 kb with an average size of 63 kb), one in a 3' UTR, and 11 not yet precisely localized. Only 13 breakpoints fell in nongenic regions. These data support the hypothesis that the chromosomal rearrangements in these phenotypically abnormal patients frequently disrupt or dysregulate a gene (or genes). Three cases revealed gene fusions that produce fusion transcripts identified by RT-PCR (DGAP011, 012, and 107). Although fusion transcripts frequently result from translocations in neoplasms, they have rarely been described in constitutional rearrangements.<sup>5</sup> The clinical significance of the fusion transcripts produced in DGAP011 and DGAP012 remain to be determined. The DGAP107 fusion transcript results in a dominant-negative ROBO2 protein that abrogates downstream signaling.<sup>20</sup>

## Discussion

In this study, we describe the most detailed analysis to date of apparently balanced chromosomal rearrangements in individuals with an abnormal phenotype. We have leveraged recent advances in the Human Genome Project and subsequent resources that have become available to localize functionally important genes on human chromosomes. In the process of uncovering these genes, we have analyzed 77 breakpoints from 40 chromosomal rearrangements, including sequence analysis of 18 of these breakpoints.

Recent reports have suggested that apparently balanced constitutional translocations in patients presenting with abnormal phenotypes may be more complex when analyzed at a higher level of resolution.<sup>16,17</sup> Our analyses revealed cryptic rearrangements in 15 of 40 (~37%) cases. The major-

ity of deletions occurred at breakpoints; however, in five cases, additional rearrangements were identified at a distance (0.2 Mb to 10 Mb) from the respective breakpoints. In DGAP107, the additional deletion was on a chromosome not involved in the reported translocation. It is reasonable to hypothesize that deletions at breakpoints may have occurred in the course of the formation of the chromosomal rearrangements. Deletions at a distance from breakpoints may be unrelated to the rearrangement, or may reflect a more complex mechanism that promotes both interchromosomal exchange and intrachromosomal deletion.

Gribble et al. reported detecting rearrangements of previously unsuspected complexity in six out of ten patients after detailed analysis of apparently balanced translocations.<sup>17</sup> We observed approximately two-thirds the rate of additional complexity as compared to this study, potentially reflecting the different patient populations analyzed. The abnormal phenotypes for the patients analyzed by Gribble et al. were largely described as learning disabilities and developmental delay.<sup>17</sup> Although we analyzed patients with these abnormalities as part of a more complex phenotype, we also analyzed patients with a greater variety of phenotypes (Figure 1 and Table 1). It also should be noted that Gribble et al. used aCGH at ~1 Mb resolution and array painting to characterize the rearrangements in their study.<sup>17</sup> Although we did analyze a subset of our rearrangements (11 cases) with aCGH, not all cases were subjected to a genome-wide assessment. However, our analyses allowed us to detect complexities at or near the breakpoints and would only have failed to uncover a rearrangement at a great distance from or in a region unrelated to the reported rearrangements. aCGH is clearly a valuable technology to complement FISH characterization of apparently balanced chromosomal rearrangements.

The mechanism of formation of these nonrecurrent chromosomal rearrangements is still unknown. Reciprocal translocations may be the result of two random double-strand breaks followed by ligation repair of these breaks by homologous recombination or nonhomologous end joining (NHEJ). For those rearrangements without



**Table 4. Breakpoint Localization and Sequence Analysis**

Case No.	Rearrangement t(a;b) or inv(ab)	Site on der(a)	Site on der(b)	Sequence Changes
DGAP003	t(3;17)(p14.3;q24.3)	Intron 25 of <i>CACNA2D3</i>	NGR	Chr 3: 11 bp deletion Chr 17: 1 bp deletion
DGAP006	t(1;2)(p32;q11)	Intron 4 of <i>SSBP3</i>	Intron 6 of <i>TMEM87B</i>	
DGAP011	t(7;8)(p12.3;p11.2)	Intron 15 of <i>TNS3</i>	Intron 2 of <i>FGFR1</i>	balanced
DGAP012	t(11;19)(p11.2;p13.3)	Intron 16 of <i>PHF21A</i>	Intron 5 of <i>ELAV</i>	Chr 11: 5 bp deletion Chr 19: 5 bp deletion
DGAP015	t(10;13)(q23.3;q33)	<i>PTEN</i>		
DGAP016	t(8;10)(p11.2;p13)	NGR	<i>NMT2</i>	
DGAP025	t(X;15)(p22;q26)	NGR	Intron 18 of <i>CHD2</i>	
DGAP032	t(7;12)(q21.13;q24)	NGR	Intron 2 of <i>RMST</i>	Chr 7: 3 bp deletion Chr 12: 17 bp insertion
DGAP089	t(1;2)(p31.3;q22.1), del(2)(q14.3q21)	Intron 7 of <i>NFIA</i>	NGR	
DGAP090	t(8;9)(q12.1;p21.3), t(9;11)(q33;q13)mat	NGR	Intron 5 of <i>MTAP</i>	Chr 8: 3 bp duplication Chr 9: 7 bp deletion, 12 bp insertion, 13 bp duplication
DGAP095	t(X;2)(p11.2;q37)	NGR	Intron 1 of <i>DGKD</i>	
DGAP097	t(X;9)(p22.2;p13)	Intron 5 of <i>CXORF15</i>	NGR	Chr X: 2 bp insertion Chr 9: 7 bp deletion, 2 bp insertion
DGAP100	t(X;5)(p11.3;q35)	Intron 2 of <i>UTX</i>		
DGAP101	inv(5)(q13q15)	Intron 2 of <i>C5ORF36</i>		
DGAP103	inv(12)(p11.22q14.3)	NGR	Intron 3 of <i>HMG2</i>	
DGAP104	t(1;20)(p31.3;q13.31)	Intron 2 of <i>NFIA</i>	Intron 2 of <i>C20ORF32</i>	
DGAP105	t(1;5)(p35.3;q31.3)	Intron 1 of <i>AHDC1</i>	3'UTR of <i>MATR3</i>	Chr 1: 16 bp deletion Chr 5: 7 bp insertion Chr Y: no change Chr 3: 1 bp deletion, 2 bp insertion
DGAP107	t(Y;3)(p11.2;p12.3)	Intron 1 of <i>PCDH11Y</i>	Intron 2 of <i>ROBO2</i>	
DGAP112	t(3;12)(q13.2;q14) del(12)(q14q14)		<i>SLC16A7</i>	
DGAP121	t(5;13)(q15;q32)	NGR	<i>DOCK9</i>	
DGAP123	ins(16;2)(q22.1;p16.1p16.3)	Intron 5 of <i>NRXN1</i>	NGR	
DGAP127	t(X;5)(q24;q13)	<i>MBNL3</i>	<i>GPR98</i>	
DGAP128	t(1;3)(q32.2;q25.2)	Intron 3 of <i>SYT14</i>	NGR	
DGAP151	t(2;8)(q33.1;q24.3)	Intron 2 of <i>SUMO1</i>	NGR	Chr 2: 9 bp deletion, 29 bp insertion Chr 8: no change
DGAP157	t(3;10)(p26.3;q26.3)		<i>ANK3</i>	
DGAP166	inv(2)(p23q31)		<i>SCN1A</i>	
DGAP174	t(1;3)(p22;q21,del(1) (p31.3p32.1)	<i>NEGR1</i>		

NGR denotes nongenic region.

sequence similarity at the breakpoints, NHEJ may be involved in translocation formation because additional genomic alterations such as small deletions, insertions, or duplications at the breakpoint junctions have been detected.<sup>25–27</sup>

Few constitutional rearrangements have been examined at the sequence level to elucidate possible mechanisms of formation.<sup>24,28</sup> Examination of 18 breakpoints sequenced in this study revealed one case with no loss or gain of material at the breakpoint junction and the majority with small duplications, insertions, and deletions. These data would suggest a mechanism of NHEJ in the formation of these rearrangements. Only one case, DGAP095, exhibited at both breakpoints a degree of sequence similarity (AluSx sequence) that may have mediated formation of the translocation. Although analyses of the breakpoints did not uncover a specific sequence or motif that would support a hy-

pothesis for a mechanism of formation, these data may be a valuable first step to future studies to elucidate a mechanism (or mechanisms) of chromosomal rearrangement.

Cases that revealed greater karyotypic complexity (Table 2) may be the result of a different mechanistic origin. The large deletions found at and away from the breakpoints could result from chromosomal pulverization at the site of rearrangement rather than the more precise double-strand breaks described above. Repair of these fragmented chromosomes could result in the large deletions observed. Recent analyses of cancer cell lines and a bone-marrow specimen from a patient with myeloproliferative disorder demonstrate deletions both at the breakpoints and at a site distant from the breakpoints.<sup>29–31</sup>

DGAP affords a unique opportunity to discover genes involved in developmental processes that otherwise could be

difficult or essentially impossible to identify;<sup>2,19,20,32–35</sup> mutations in some of these genes may not be found segregating as Mendelian traits in human families because affected individuals may have a genetic fitness of zero. In keeping with the overarching goal of gene discovery in the DGAP study, genes were found to be disrupted at 34 breakpoints. Seven candidate genes have functions that remain to be investigated.

In addition to identifying new genes, this gene-discovery approach may uncover known genes with previously unappreciated roles in developmental pathways. Examples include *SUMO1* (MIM 601912) in palatal development,<sup>19</sup> *ROBO2* (MIM 602431) in urinary tract development,<sup>20</sup> and *NFIA* (MIM 600727) in urinary tract and central nervous system development.<sup>23</sup> Thus far, we have shown disrupted genes to be contributory to the patient's phenotype in 12 cases (Table 1).

Our data support the hypothesis that apparently balanced chromosomal rearrangements are valuable biological landmarks for genes important in human development. Although cryptic genomic disturbances may also be observed in individuals with congenital anomalies and apparently balanced rearrangements by conventional cytogenetics, their presence does not necessarily diminish the value of a particular case in contributing to the understanding of the genetic basis of a developmental disorder.<sup>20,23</sup> In sum, naturally occurring chromosomal rearrangements continue to be a rich resource for gene discovery and annotation.

## Supplemental Data

The sequence of DGAP cases analyzed for motifs can be found with this article online at <http://www.ajhg.org/>.

## Acknowledgments

We wish to express our sincere gratitude to all the patients and their families who are enrolled in DGAP, and to the many genetic counselors, clinical geneticists, and cytogeneticists who have made this effort possible; to Dr. Charles Lee for his assistance with M-FISH; and to the Dana-Farber/Harvard Cancer Center (DF/HCC) Cytogenetics Core (P30CA06516) for assistance with the array CGH. This study was supported by National Institutes of Health grants P01 GM061354 (to C.C.M.), F32 HD043627 (to N.T.L.), F31 DC005712 (to R.E.W.), and F31 DC007540 (to K.K.B.); by a Children's Tumor Foundation Young Investigator Award (to Y.S.); and by a National Kidney Foundation Young Investigator Grant and the Evans Medical Foundation (to W.L.).

Received: October 19, 2007

Revised: December 17, 2007

Accepted: January 4, 2008

Published online: March 6, 2008

## Web Resources

The URLs for data presented herein are as follows:

Developmental Genome Anatomy Project (DGAP), <http://dgap.harvard.edu>

NCBI Human Genome Browser and Database, <http://www.ncbi.nlm.nih.gov>

Online Mendelian Inheritance in Man (OMIM), <http://www.ncbi.nlm.nih.gov/Omim/>

Repeat Masker, <http://www.repeatmasker.org/>

University of California Santa Cruz Genome Browser and Database, <http://genome.ucsc.edu>

YMF 3.0 motif-finding tool, <http://wingless.cs.washington.edu/YMF>

## References

- Warburton, D. (1991). De novo balanced chromosome rearrangements and extra marker chromosomes identified at prenatal diagnosis: Clinical significance and distribution of breakpoints. *Am. J. Hum. Genet.* 49, 995–1013.
- Kim, H.G., Herrick, S.R., Lemyre, E., Kishikawa, S., Salisz, J.A., Seminara, S., MacDonald, M.E., Bruns, G.A., Morton, C.C., Quade, B.J., et al. (2005). Hypogonadotropic hypogonadism and cleft lip and palate caused by a balanced translocation producing haploinsufficiency for FGFR1. *J. Med. Genet.* 42, 666–672.
- Ligon, A.H., Moore, S.D., Parisi, M.A., Mealiffe, M.E., Harris, D.J., Ferguson, H.L., Quade, B.J., and Morton, C.C. (2005). Constitutional rearrangement of the architectural factor HMGA2: A novel human phenotype including overgrowth and lipomas. *Am. J. Hum. Genet.* 76, 340–348.
- Menten, B., Maas, N., Thienpont, B., Buysse, K., Vandesompele, J., Melotte, C., de Ravel, T., Van Vooren, S., Balikova, I., Backx, L., et al. (2006). Emerging patterns of cryptic chromosomal imbalance in patients with idiopathic mental retardation and multiple congenital anomalies: A new series of 140 patients and review of published reports. *J. Med. Genet.* 43, 625–633.
- Nothwang, H.G., Kim, H.G., Aoki, J., Geisterfer, M., Kubart, S., Wegner, R.D., van Moers, A., Ashworth, L.K., Haaf, T., Bell, J., et al. (2001). Functional hemizyosity of PAFAH1B3 due to a PAFAH1B3–CLK2 fusion gene in a female with mental retardation, ataxia and atrophy of the brain. *Hum. Mol. Genet.* 10, 797–806.
- Kleinjan, D.J., and van Heyningen, V. (1998). Position effect in human genetic disease. *Hum. Mol. Genet.* 7, 1611–1618.
- Dermitzakis, E.T., Reymond, A., and Antonarakis, S.E. (2005). Conserved non-genic sequences - an unexpected feature of Mamm. Genomes. *Nat. Rev. Genet.* 6, 151–157.
- Mattick, J.S. (2005). The functional genomics of noncoding RNA. *Science* 309, 1527–1528.
- Ray, P.N., Belfall, B., Duff, C., Logan, C., Kean, V., Thompson, M.W., Sylvester, J.E., Gorski, J.L., Schmickel, R.D., and Worton, R.G. (1985). Cloning of the breakpoint of an X;21 translocation associated with Duchenne muscular dystrophy. *Nature* 318, 672–675.
- Ishikiriya, S., Tonoki, H., Shibuya, Y., Chin, S., Harada, N., Abe, K., and Niikawa, N. (1989). Waardenburg syndrome type I in a child with de novo inversion (2)(q35q37.3). *Am. J. Med. Genet.* 33, 505–507.
- Viskochil, D., Buchberg, A.M., Xu, G., Cawthon, R.M., Stevens, J., Wolff, R.K., Culver, M., Carey, J.C., Copeland, N.G., Jenkins, N.A., et al. (1990). Deletions and a translocation interrupt a cloned gene at the neurofibromatosis type 1 locus. *Cell* 62, 187–192.

12. Spinner, N.B., Rand, E.B., Fortina, P., Genin, A., Taub, R., Semeraro, A., and Piccoli, D.A. (1994). Cytologically balanced t(2;20) in a two-generation family with Alagille syndrome: Cytogenetic and molecular studies. *Am. J. Hum. Genet.* 55, 238–243.
13. Tommerup, N., van der Hagen, C.B., and Heiberg, A. (1992). Tentative assignment of a locus for Rubinstein-Taybi syndrome to 16p13.3 by a de novo reciprocal translocation, t(7;16)(q34;p13.3). *Am. J. Med. Genet.* 44, 237–241.
14. Tonkin, E.T., Wang, T.J., Lisgo, S., Bamshad, M.J., and Strachan, T. (2004). NIPBL, encoding a homolog of fungal Scc2-type sister chromatid cohesion proteins and fly Nipped-B, is mutated in Cornelia de Lange syndrome. *Nat. Genet.* 36, 636–641.
15. Johnson, D., Morrison, N., Grant, L., Turner, T., Fantes, J., Connor, J.M., and Murday, V. (2006). Confirmation of CHD7 as a cause of CHARGE association identified by mapping a balanced chromosome translocation in affected monozygotic twins. *J. Med. Genet.* 43, 280–284.
16. Astbury, C., Christ, L.A., Aughton, D.J., Cassidy, S.B., Kumar, A., Eichler, E.E., and Schwartz, S. (2004). Detection of deletions in de novo “balanced” chromosome rearrangements: Further evidence for their role in phenotypic abnormalities. *Genet. Med.* 6, 81–89.
17. Gribble, S.M., Prigmore, E., Burford, D.C., Porter, K.M., Ng, B.L., Douglas, E.J., Fiegler, H., Carr, P., Kalaitzopoulos, D., Clegg, S., et al. (2005). The complex nature of constitutional de novo apparently balanced translocations in patients presenting with abnormal phenotypes. *J. Med. Genet.* 42, 8–16.
18. Siebert, P.D., Chenchik, A., Kellogg, D.E., Lukyanov, K.A., and Lukyanov, S.A. (1995). An improved PCR method for walking in uncloned genomic DNA. *Nucleic Acids Res.* 23, 1087–1088.
19. Alkuraya, F.S., Saadi, I., Lund, J.J., Turbe-Doan, A., Morton, C.C., and Maas, R.L. (2006). SUMO1 haploinsufficiency leads to cleft lip and palate. *Science* 313, 1751.
20. Lu, W., van Eerde, A.M., Fan, X., Quintero-Rivera, F., Kulkarni, S., Ferguson, H., Kim, H.G., Fan, Y., Xi, Q., Li, Q.G., et al. (2007). Disruption of ROBO2 is associated with urinary tract anomalies and confers risk of vesicoureteral reflux. *Am. J. Hum. Genet.* 80, 616–632.
21. Abo-Dalo, B., Kim, H.G., Roes, M., Stefano, M., Higgins, A.W., Shen, Y., Mundlos, S., Quade, B.J., Gusella, J.F., and Kutsche, K. (2007). Extensive molecular genetic analysis of the 3p14.3 region in patients with Zimmermann-Laband syndrome. *Am. J. Med. Genet. A* 143, 2668–2674.
22. Shanske, A.L., Edelmann, L., Kardon, N.B., Gosset, P., and Levy, B. (2004). Detection of an interstitial deletion of 2q21–22 by high resolution comparative genomic hybridization in a child with multiple congenital anomalies and an apparent balanced translocation. *Am. J. Med. Genet. A* 131, 29–35.
23. Lu, W., Quintero-Rivera, F., Fan, Y., Alkuraya, F.S., Donovan, D.J., Xi, Q., Turbe-Doan, A., Li, Q.G., Campbell, C.G., Shanske, A.L., et al. (2007). NFIA haploinsufficiency is associated with a CNS malformation syndrome and urinary tract defects. *PLoS Genet.* 3, e80.
24. Abeyasinghe, S.S., Chuzhanova, N., Krawczak, M., Ball, E.V., and Cooper, D.N. (2003). Translocation and gross deletion breakpoints in human inherited disease and cancer I: Nucleotide composition and recombination-associated motifs. *Hum. Mutat.* 22, 229–244.
25. Jeggo, P.A. (1998). DNA breakage and repair. *Adv. Genet.* 38, 185–218.
26. Sargent, R.G., Brenneman, M.A., and Wilson, J.H. (1997). Repair of site-specific double-strand breaks in a mammalian chromosome by homologous and illegitimate recombination. *Mol. Cell. Biol.* 17, 267–277.
27. Pfeiffer, P., Goedecke, W., and Obe, G. (2000). Mechanisms of DNA double-strand break repair and their potential to induce chromosomal aberrations. *Mutagenesis* 15, 289–302.
28. GajECKa, M., PavliceK, A., Glotzbach, C.D., Ballif, B.C., Jarmuz, M., Jurka, J., and Shaffer, L.G. (2006). Identification of sequence motifs at the breakpoint junctions in three t(1;9)(p36.3;q34) and delineation of mechanisms involved in generating balanced translocations. *Hum. Genet.* 120, 519–526.
29. Mao, X., James, S.Y., Yanez-Munoz, R.J., Chaplin, T., Molloy, G., Oliver, R.T., Young, B.D., and Lu, Y.J. (2007). Rapid high-resolution karyotyping with precise identification of chromosome breakpoints. *Genes Chromosomes Cancer* 46, 675–683.
30. Watson, S.K., deLeeuw, R.J., Horsman, D.E., Squire, J.A., and Lam, W.L. (2007). Cytogenetically balanced translocations are associated with focal copy number alterations. *Hum. Genet.* 120, 795–805.
31. Etienne, A., Carbuccia, N., Adelaide, J., Bekhouche, I., Remy, V., Sohn, C., Sainty, D., Gastaut, J.-A., Olschwang, S., Birnbaum, D., et al. (2007). Rearrangements involving 12q in myeloproliferative disorders: Possible role of *HMGA2* and *SOC32* gene. *Cancer Genet. Cytogenet.* 176, 80–88.
32. Leach, N.T., Sun, Y., Michaud, S., Zheng, Y., Ligon, K.L., Ligon, A.H., Sander, T., Korf, B.R., Lu, W., Harris, D.J., et al. (2007). Disruption of diacylglycerol kinase delta (DGKD) associated with seizures in humans and mice. *Am. J. Hum. Genet.* 80, 792–799.
33. Kim, H.G., Higgins, A.W., Herrick, S.R., Kishikawa, S., Nicholson, L., Kutsche, K., Ligon, A.H., Harris, D.J., Macdonald, M.E., Bruns, G.A., et al. (2007). Candidate loci for Zimmermann-Laband syndrome at 3p14.3. *Am. J. Med. Genet. A* 143, 107–111.
34. Williamson, R.E., Darrow, K.N., Michaud, S., Jacobs, J.S., Jones, M.C., Eberl, D.F., Maas, R.L., Liberman, M.C., and Morton, C.C. (2007). Methylthioadenosine phosphorylase (MTAP) in hearing: Gene disruption by chromosomal rearrangement in a hearing impaired individual and model organism analysis. *Am. J. Med. Genet. A* 143A, 1630–1639.
35. Quintero-Rivera, F., Chan, A., Donovan, D.J., Gusella, J.F., and Ligon, A.H. (2007). Disruption of a synaptotagmin (SYT14) associated with neurodevelopmental abnormalities. *Am. J. Med. Genet. A* 143, 558–563.
36. Kim, H.-G., Kishikawa, S., Higgins, A.W., Seong, I.-S., Donovan, D.J., Shen, Y., Lally, E., Weiss, L.A., Najm, J., Kutsche, K., et al. (2007). Disruption of neurexin 1 associated with autism spectrum disorder. *Am. J. Hum. Genet.* 82, 199–207.